

# Efficiency Modeling and Performance Comparison of Switched Capacitor Converter EV/PHEV Drives

Zahra Amjadi, *Student Member, IEEE*, and Sheldon S. Williamson, *Member, IEEE*

Power Electronics and Energy Research (PEER) Group  
P. D. Ziogas Power Electronics Laboratory  
Department of Electrical and Computer Engineering  
Concordia University  
1455 de Maisonneuve Blvd. W.  
Montreal, Quebec H3G 1M8, Canada  
Phone: +1/(514) 848-2424, ext. 8741  
EML: [sheldon@ece.concordia.ca](mailto:sheldon@ece.concordia.ca)  
URL: <http://www.ece.concordia.ca/~peer/>

**Abstract**– This paper presents the performance comparison and transfer efficiency modeling and analysis of a 4-quadrant switched capacitor Luo (4-Q SC Luo) converter and 2-Q SCC, applicable for hybrid electric and plug-in hybrid electric vehicles (PHEV) Energy storage system (ESS) applications. Features of voltage step-down, voltage step-up, and bi-directional power flow are integrated into a single circuit. The SCC enables simpler dynamics compared to a standard buck converter, with input filter, good regulation capability, low EMI, lower source current ripple, ease of control, and continuous input current waveform in both modes of operation (buck and boost modes).

## I. INTRODUCTION

Due to their practicality, the leading future vehicle technology options in the short term include the hybrid electric vehicle (HEV) and plug-in hybrid electric vehicle (PHEV). Hybrid energy storage systems (parallel batteries and Ultra-capacitors) are usually employed in PHEVs to reduce the overall cost, size, and weight of the vehicle and improve performance. Ultra-capacitors (UC's) consist of high dynamics and a lifespan of about 10 years higher than that of batteries. The UC's have a power density ranging from 10 to 100 times larger than that of batteries. In general, the UC bank is used for satisfying acceleration and regenerative braking requirements. In addition, it also helps to improve the on-board battery life time. The combination of battery and UC results in reduced size and weight of the overall energy storage system (ESS) [1], [2].

A switched capacitor converter (SCC) is essentially a combination of switches and capacitors. The different combinations of capacitors and switches results in SCC topologies producing an output voltage that may be higher (boost mode) or lower (buck mode) than the input voltage as well as polarity reversal. The switches are controlled by capacitors that they are charged and discharged through different paths. Switched-capacitor (SC) bidirectional converters, with their large voltage conversion ratio, indeed possess the potential to be one of the possible solutions for

achieving high-efficiency conversion for HEV energy storage systems. At the same time, SCCs possess the ability to realize step up/down of voltage. [3] - [8].

This paper initially discusses on operational analysis of a bidirectional DC/DC SCC and its efficiency modeling and analysis and then goes on SC Luo converter operating characteristics and modes and its transfer efficiency.

## II. OPERATIONAL ANALYSIS OF A BIDIRECTIONAL DC/DC SWITCHED CAPACITOR CONVERTER

A bidirectional SCC is shown in Fig. 1. It consists of 4 switches, 4 diodes, and one capacitor. In both (SCC and SC Luo) converters, high voltage (HV) side consists of the on-board battery modules and the low voltage (LV) side consists of UC modules.

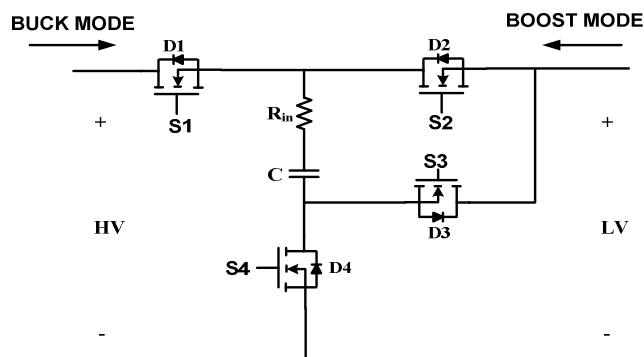


Fig. 1. A bidirectional DC/DC switched capacitor converter.

There are 2 basic modes of operation; mode A (quadrant I): electrical energy is transferred from HV side to LV side; mode B (quadrant II): electrical energy is transferred from LV side to HV side.

### Circuit Description

Each mode has 2 states: *on* and *off*. Usually, each state operates with a different conduction duty,  $k$ . The switching period is  $T$ , where  $T = 1/f$ . The parasitic resistance of all switches is  $r_s$  and the equivalent resistance of the capacitor is  $r_c$ .

#### a) Mode A (Buck Operation)

For mode A, state-on is shown in Fig. 2 (a). Switches  $S_1$  and  $S_4$  are closed and capacitor C is charged by HV side or battery modules and voltage across capacitor C increases. The equivalent circuit resistance is  $R_{AN} = r_{s1} + r_{s4} + r_c$ . Other switches and diodes are open. State-off is shown in Fig. 2 (b). Switch  $S_2$  is closed and  $D_4$  starts conducting, while capacitor C is disconnected from HV side and transfers its stored energy to LV side; the voltage across capacitor C is decreases. The equivalent circuit resistance is  $R_{Af} = r_{s2} + r_c$  [9]-[14].

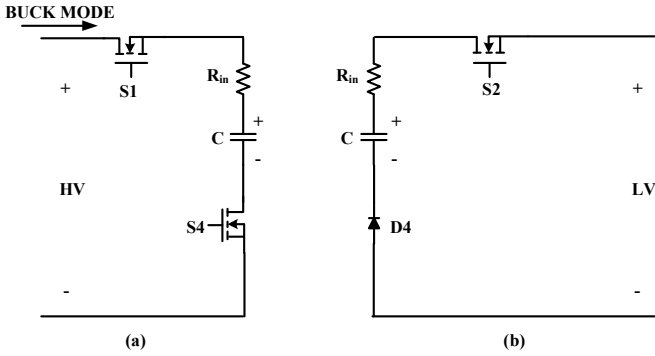


Fig. 2. Buck mode (a) capacitor C is charged and is connected to HV side, (b) capacitor C is discharged and is disconnected from HV side.

If the switching period  $T$  is small enough (compared to the circuit time constant), an average current may be used to replace its instantaneous value, for the purpose of integration. Therefore, the voltage across capacitor C is:

$$V_C(t) = \begin{cases} V_C(0) + \frac{1}{C} \int_0^t I_C(t) dt \approx V_C(0) + \frac{t}{C} \overline{I_H} & 0 \leq t \leq kT \\ V_C(kT) + \frac{1}{C} \int_{kT}^t I_C(t) dt \approx V_C(kT) - \frac{t-kT}{C} \overline{I_L} & kT \leq t \leq T \end{cases} \quad (1)$$

If the switching period  $T$  is small enough (compared to the circuit time constant), their initial values may be used, while ignoring trivial variations. Therefore, the current flowing through capacitor C is:

$$I_C(t) = \begin{cases} \frac{V_H - V_C}{R_{AN}} = \overline{I_H} & 0 \leq t \leq kT \\ -\frac{-V_L + V_C - V_{D4}}{R_{Af}} = -\overline{I_L} & kT \leq t \leq T \end{cases} \quad (2)$$

Where  $\overline{I_H}$  is the average input current in the switch-on period  $kT$ , and  $\overline{I_L}$  is the average output current in the switch-off period  $(1-k)T$ . The variation of the voltage across capacitor C is:

$$\Delta V_C = \begin{cases} \frac{1}{C} \int_0^{kT} I_C(t) dt = \frac{kT}{C} \overline{I_H} & 0 \leq t \leq kT \\ \frac{1}{C} \int_{kT}^T I_C(t) dt = \frac{(1-k)T}{C} \overline{I_L} & kT \leq t \leq T \end{cases} \quad (3)$$

Also, voltage across capacitor C after calculation is:

$$V_C = \frac{kR_{Af}V_H + (1-k)R_{AN}(V_L + V_{D4})}{(1-k)R_{AN} + kR_{Af}} \quad (4)$$

Hence,

$$\Delta V_C = \frac{k(1-k)[V_H - (V_L + V_{D4})]}{fC((1-k)R_{AN} + kR_{Af})} \quad (5)$$

The average input current is:

$$I_H = \frac{1}{T} \int_0^{kT} I_C(t) dt = k \frac{V_H - V_C}{R_{AN}} \quad (6)$$

The average output current is:

$$I_L = \frac{1}{T} \int_{kT}^T I_C(t) dt = (1-k) \frac{-V_L + V_C - V_{D4}}{R_{Af}} \quad (7)$$

The transfer efficiency is:

$$\eta = \frac{P_O}{P_I} = \frac{V_L * (1-k) * (-V_L + V_C - V_{D4}) * R_{AN}}{V_H * k * (V_H - V_C) * R_{Af}} \quad (8)$$

#### b) Mode B (Boost Operation)

For mode B, state-on is shown in Fig. 3 (a). Switch  $S_4$  is closed and  $D_2$  starts conducting; capacitor C is charged by LV side and voltage across capacitor C increases. The equivalent circuit resistance is  $R_{BN} = r_{s4} + r_c$ . Other switches and diodes are open. State-off is shown in Fig. 3 (b). Switch  $S_3$  is closed and  $D_1$  starts conducting; capacitor C is connected in series with the LV side and is discharged, whereby it supplies its energy to the HV side and voltage across capacitor C decreases. The equivalent circuit resistance is  $R_{Bf} = r_{s3} + r_c$  [9]-[14].

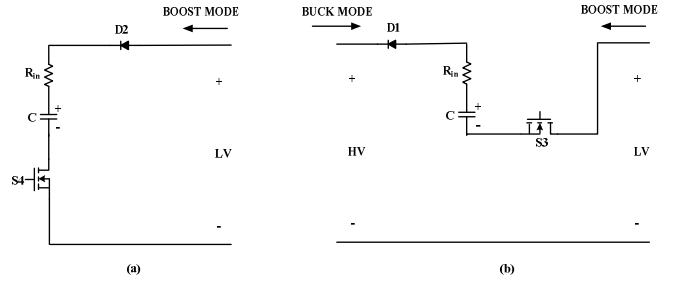


Fig. 3. Boost mode (a) capacitor C is charged, (b) capacitor C is discharged and is connected in series with the LV side.

If the switching period  $T$  is small enough (compared to the circuit time constant), the average current can be used to replace its instantaneous value for integration. Therefore, the voltage across capacitor C is:

$$V_C(t) = \begin{cases} V_C(0) + \frac{1}{C} \int_0^t I_C(t) dt \approx V_C(0) + \frac{t}{C} \overline{I_L} & 0 \leq t \leq kT \\ V_C(kT) + \frac{1}{C} \int_{kT}^t I_C(t) dt \approx V_C(kT) - \frac{t-kT}{C} \overline{I_H} & kT \leq t \leq T \end{cases} \quad (9)$$

If the switching period  $T$  is small enough (compared to the circuit time constant), their initial values can be used, while ignoring their variations. Therefore the current flowing through capacitor  $C$  is:

$$I_C(t) = \begin{cases} \frac{V_L - V_C - V_{D2}}{R_{BN}} = \overline{I_L} & 0 \leq t \leq kT \\ -\frac{V_H + V_C - V_{D1} + V_L}{R_{Bf}} = -\overline{I_H} & kT \leq t \leq T \end{cases} \quad (10)$$

Here,  $\overline{I_L}$  is the average input current in the switch-on period  $kT$ , and  $\overline{I_H}$  is the average output current in the switch-off period  $(1-k)T$ . The variation of the voltage across capacitor  $C$  is:

$$\Delta V_C = \begin{cases} \frac{1}{C} \int_0^{kT} I_C(t) dt = \frac{k}{Cf} * \frac{V_L - V_C - V_{D2}}{R_{BN}} & 0 \leq t \leq kT \\ \frac{1}{C} \int_{kT}^T I_C(t) dt = \frac{(1-k)}{Cf} * \frac{-V_H + V_C - V_{D1} + V_L}{R_{Bf}} & kT \leq t \leq T \end{cases} \quad (11)$$

Also, voltage across capacitor  $C$  after calculation is:

$$V_C = \frac{kR_{Bf}(V_L - V_{D2}) + (1-k)R_{BN}(V_H - V_L + V_{D1})}{(1-k)R_{BN} + kR_{Bf}} \quad (12)$$

The average input current is:

$$I_L = \frac{1}{T} \left[ \int_0^{kT} I_C(t) dt + \int_{kT}^T I_C(t) dt \right] = k \left( \frac{V_L - V_C - V_{D2}}{R_{BN}} \right) + (1-k) \frac{V_L + V_C - V_H - V_{D1}}{R_{Bf}} \quad (13)$$

The average output current is:

$$I_H = \frac{1}{T} \int_{kT}^T I_C(t) dt = (1-k) \frac{V_L + V_C - V_H - V_{D1}}{R_{Bf}} \quad (14)$$

The transfer efficiency is:

$$\eta = \frac{P_O}{P_I} = \frac{V_H * [(1-k) \left( \frac{V_L + V_C - V_H - V_{D1}}{R_{Bf}} \right)]}{V_L * \left[ k \left( \frac{V_L - V_C - V_{D2}}{R_{BN}} \right) + (1-k) \frac{V_L + V_C - V_H - V_{D1}}{R_{Bf}} \right]} \quad (15)$$

The transfer efficiency is independent upon  $R$ ,  $C$ ,  $f$ , and  $k$ . The conduction duty  $k$  does not affect the transfer efficiency but does affect the input and output power in a diminutive operating window.

In this particular circuit, transfer efficiency in buck mode, with total battery voltage 60V and UC voltage 21.9V, is computed to be about 68.5%, and in boost mode, with total battery voltage 59.9V and UC voltage 35V, is computed to be around 85%.

### III. CONTROLLER DESIGN FOR SC LUO CONVERTER OPERATION

A typical system schematic is shown in Fig. 4, consisting of a SC *Lu*o based bi-directional DC/DC energy management converter.

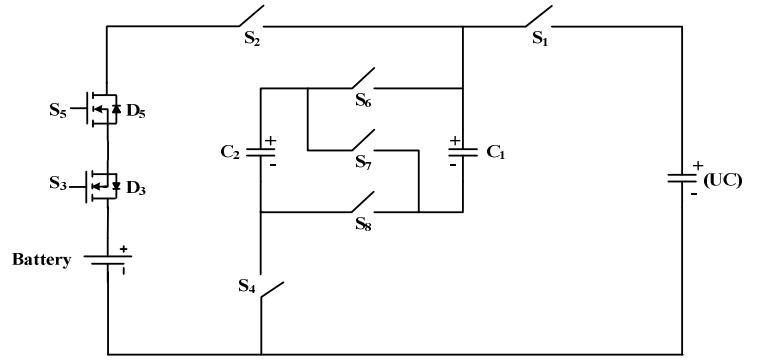


Fig. 4. Layout of a 4-Q SC *Lu*o converter for HEV applications.

The 4-Q SC *Lu*o converter is comprised of 6 switches and 2 capacitors,  $C_1$  and  $C_2$ . Each switch consists of two MOSFETs, for current flow in both directions. In this case, the high voltage DC is at 86V, low voltage side is set at 43V, and UC initial voltage is at 22V. This type of converter operates in four quadrants (forward and reverse mode). Fig. 5 shows the complete system schematic.

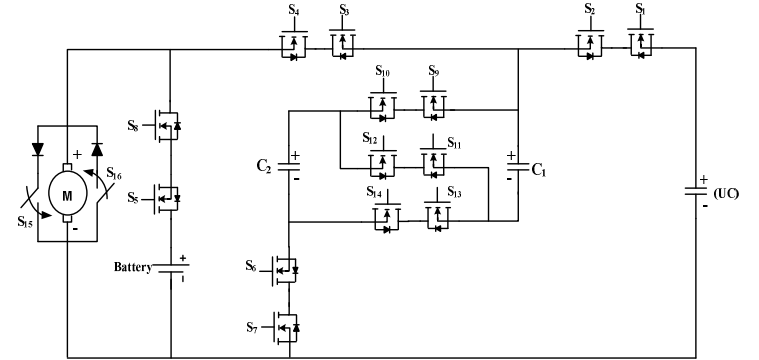


Fig. 5. Circuit schematic with hybrid energy sources and traction motor.

When the converter operates in motoring mode ( $P \geq 0$ ), two conditions are chosen: If the battery current gradient is between -2mA and 2mA, battery modules supply their energy to the load and motor side. Otherwise, UC modules supply their power to load and motor side. Secondly, during motoring mode, output power of motor ( $P_{out}$ ) is compared with load power ( $P_L$ ). If  $P_{out} < P_L$ , with attention given to battery current gradient, UC or battery modules supply their power to the motor side. Otherwise, if the battery modules need energy and fully discharge, the UC modules transfer their power to battery or HV side. If the UC modules need energy and fully discharge, the battery modules deliver their energy to UC or LV side. On the other hand, when the converter operates in generating mode ( $P < 0$ ), only the first condition is considered. In generating mode, the motor tends to give up its power; thus it is not compared with load power.

#### IV. SC LUO CONVERTER OPERATING CHARACTERISTICS AND MODES

In forward motoring or quadrant I operation, voltage and current are positive. At the same time, if  $P_{out} < P_L$ , the UC and battery modules supply their power to motor side with attention given to the battery current gradient. Otherwise, battery or UC modules deliver their energy between each other. For better understanding of the controller, each operation mode is denoted by a specific code.

When  $P_{out} < P_L$ , and UC modules transfer their power to motor, switches  $S_2$  and  $S_4$  are closed and  $D_1$  and  $D_3$  start conducting. This mode is represented with code 1, as shown in Fig. 6 (a). However, when battery modules deliver their energy to motor side, switch  $S_5$  is closed and  $D_8$  starts conducting. This mode is shown by code 2, and is depicted in Fig. 6 (b).

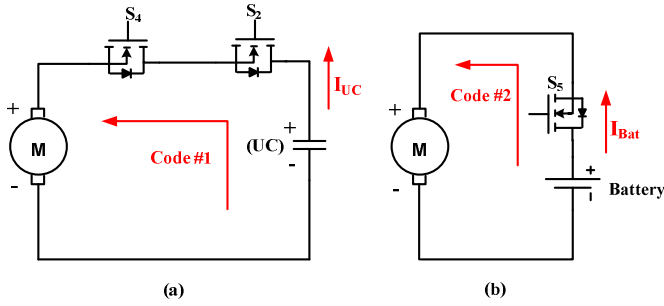


Fig. 6. Forward motoring (a) UC modules, (b) Battery modules supply their power to motor side.

Now, if  $P_{out} \geq P_L$ , and battery modules are fully discharged, LV side or UC modules transfer their power to HV side, as a first step. Switches  $S_2$ ,  $S_{10}$ ,  $S_{14}$ , and  $S_7$  are on, and  $D_1$ ,  $D_9$ ,  $D_{13}$ , and  $D_6$  start conducting. Capacitors  $C_1$  and  $C_2$  are charged by the LV side. Also, the voltage across the 2 capacitors increases. This mode is represented by code 3. The operation mode is shown in Fig. 7 (a). Also, in both operation modes (buck and boost modes),  $S_{16}$  is on, because motor does not stop and current flows through the armature.

After this operating stage,  $S_6$ ,  $S_{11}$ ,  $S_4$  and  $S_8$  are on, and  $D_7$ ,  $D_{12}$ ,  $D_3$ , and  $D_5$  start conducting. Capacitors  $C_1$  and  $C_2$  are disconnected from LV side and transfer their stored energy to the HV side. Also, the voltage across the 2 capacitors decreases. This mode is shown by code 4. The boost mode implements the *voltage-lift technique*, because the capacitors are charged during the on-state. The input voltage (LV) appears across to the capacitors. The capacitors are discharged in series during the off-state. Hence, through this straightforward method, output voltage can be boosted by the capacitors. This operation mode is depicted in Fig. 7 (b).

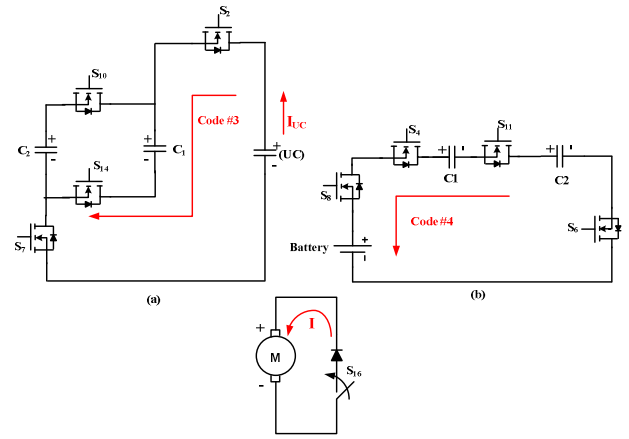


Fig. 7. In boost operation; (a) Capacitors  $C_1$  and  $C_2$  are charged by LV side; (b) Capacitors are discharged and are disconnected from LV side ( $S_{16}$  is on and current flows in motor).

Now, if  $P_{out} \geq P_L$ , and UC modules are fully discharged, battery modules transfer their energy to the LV side, as a first step. Switches  $S_5$ ,  $S_3$ ,  $S_{12}$ , and  $S_7$  are on, and  $D_8$ ,  $D_4$ ,  $D_{11}$ , and  $D_6$  start conducting. Capacitors  $C_1$  and  $C_2$  are charged by HV side. Also, the voltage across the 2 capacitors increases. This mode is represented by code 10. This operation mode is shown in Fig. 8 (a).

After this operating stage,  $S_6$ ,  $S_9$ ,  $S_{13}$  and  $S_1$  are on, and  $D_7$ ,  $D_{10}$ ,  $D_{14}$ , and  $D_2$  start conducting. Capacitors  $C_1$  and  $C_2$  are disconnected from HV side and transfer their stored energy to the LV side. Also, the voltage across the 2 capacitors decreases. This mode is shown by code 11. The buck mode uses the *current-amplification technique*, because the capacitors are charged during on-state. The input current flows through capacitors. These capacitors are discharged during off-state in parallel. Therefore, the output current is amplified by these capacitors [15]-[18]. This operation mode is depicted in Fig. 8 (b).

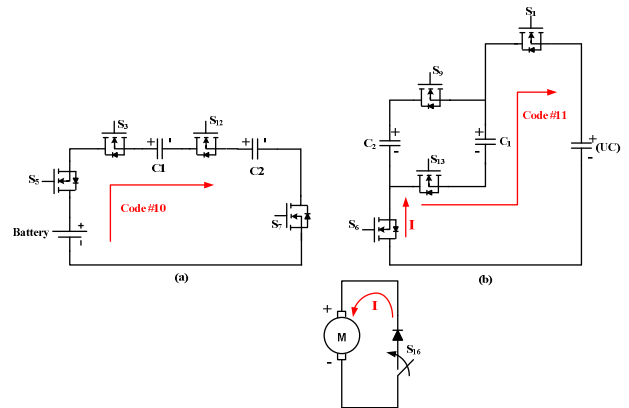


Fig. 8. In buck operation; (a) Capacitors  $C_1$  and  $C_2$  are charged by HV side; (b) Capacitors are discharged and are disconnected from HV side ( $S_{16}$  is on and current flows in motor).

If UC or battery modules are fully discharged, and  $P_{out} \geq P_L$ , then  $S_{16}$  turns on, because current flows through the motor. This mode is represented by code 9. This operation mode is shown in Fig. 9.

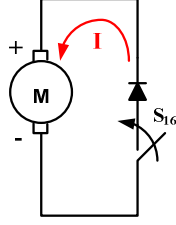


Fig. 9. Forward motoring operation; hybrid energy sources are fully discharged ( $P_{out} \geq P_L$  and  $S_{16}$  is on).

In forward regenerative (forward braking) or quadrant II operation, voltage is positive but current is negative. In this operating mode, only battery current gradient is considered. When motor supplies power to the UC side and UC modules are fully discharged or half charged, then motor transfer its power to LV side and switches  $S_3$  and  $S_1$  are closed.  $D_4$  and  $D_2$  start conducting. This mode is represented by code zero, and is shown in Fig.10 (a). When the motor supplies power to battery side, and also, battery modules are fully discharged or half charged, motor transfers its power to HV side, and switch  $S_8$  turns on.  $D_5$  starts conducting, and this mode is represented by code 5, as shown in Fig. 10 (b). However, if hybrid energy sources (battery and UC modules) are fully charged, switch  $S_{15}$  is on, because current flows through the motor. This mode is shown by code 8, and is depicted in Fig. 10 (c).

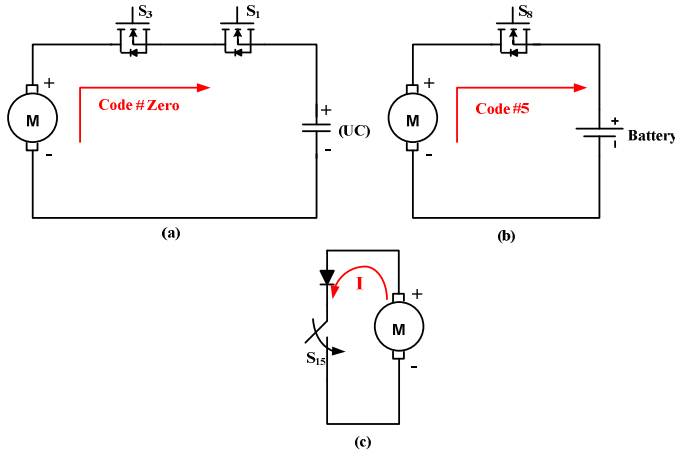


Fig. 10. Forward regenerative operation; (a) UC modules, (b) Battery modules are fully discharged or half charged; (c) hybrid energy sources are fully charged and current flows in motor.

In reverse motoring (quadrant III) operation, voltage and current are negative. This operation mode and its codes are same as forward motoring. In reverse regenerative (reverse braking or quadrant IV) operation, voltage is negative.

However, current is positive. This operation mode and its codes are same as forward regenerative.

## V. SC LUO CONVERTER EFFICIENCY MODELING AND ANALYSIS

The detailed transfer efficiency modeling and analysis of the SC Luo converter are explained in this section. As aforementioned, the SCC has 2 main modes of operation, the buck mode and boost mode.

The buck mode uses the *current-amplification technique*. If the switching period,  $T$ , is small enough (compared to the circuit time constant), an average current can be used, to replace its instantaneous value, for the purpose of integration. Also, capacitors  $C_1$  and  $C_2$  are of equal sizes, so that the voltage across each of them is equal. Therefore, the voltage across capacitor  $C_1$  can be expressed as:

$$V_C(t) = \begin{cases} V_C(0) + \frac{1}{C} \int_0^t I_C(t) dt \approx V_C(0) + \frac{t}{C} \overline{I_{Bat}} & 0 \leq t \leq kT \\ V_C(kT) + \frac{1}{C} \int_{kT}^t I_C(t) dt \approx V_C(kT) - \frac{t-kT}{2C} \overline{I_{UC}} & kT \leq t \leq T \end{cases} \quad (16)$$

If the switching period,  $T$ , is small enough (compared to the circuit time constant), initial values can be used, while ignoring trivial variations. Therefore, the current flowing through capacitor  $C_1$  can be written as:

$$I_{C1}(t) = \begin{cases} \frac{V_{Bat} - 4V_D - 2V_C}{R_{AN}} = \overline{I_{Bat}} & 0 \leq t \leq kT \\ -\frac{-V_{UC} + V_C - 3V_D}{R_{Af}} = -\frac{\overline{I_{UC}}}{2} & kT \leq t \leq T \end{cases} \quad (17)$$

Here,

$$R_{AN} = 4r_S + 2r_C \quad R_{Af} = 3r_S + r_C$$

$\overline{I_{Bat}}$  is the average input current during the switch-on period,  $kT$ , and  $\overline{I_{UC}}$  is the average output current during the switch-off period,  $(1-k)T$ . The variation of the voltage across capacitor  $C_1$  is:

$$\Delta V_C = \begin{cases} \frac{k}{C_f} * \frac{V_{Bat} - 4V_D - 2V_C}{R_{AN}} & 0 \leq t \leq kT \\ \frac{(1-k)}{C_f} * \frac{-V_{UC} + V_C - 3V_D}{2R_{Af}} & kT \leq t \leq T \end{cases} \quad (18)$$

Also, voltage across capacitor  $C_1$  can be written as:

$$V_C = \frac{2kR_{Af}(V_{Bat} - 4V_D) + (1-k)R_{AN}(V_{UC} + 3V_D)}{(1-k)R_{AN} + 4kR_{Af}} \quad (19)$$

Hence, the overall transfer efficiency can be computed as:

$$\eta = \frac{P_O}{P_I} = \frac{V_{UC} * (1-k) * (-V_{UC} + V_C - 3V_D) * R_{AN}}{V_{Bat} * k * (V_{Bat} - 4V_D - 2V_C) * R_{Af}} \quad (20)$$

During buck mode (or codes 10 and 11), the battery modules are half charged or fully charged, and UC modules are fully discharged. Therefore, transfer efficiency in buck mode, with

total battery voltage 60V and UC voltage 21.9V, is computed to be about 73%.

As aforementioned, the boost mode implements the *voltage-lift technique*. Thus, the voltage across capacitor  $C_1$  can be expressed as:

$$V_C(t) = \begin{cases} V_C(0) + \frac{1}{C} \int_0^t I_C(t) dt \approx V_C(0) + \frac{t}{2C} \overline{I_{UC}} & 0 \leq t \leq kT \\ V_C(kT) + \frac{1}{C} \int_{kT}^t I_C(t) dt \approx V_C(kT) - \frac{t-kT}{C} \overline{I_{Bat}} & kT \leq t \leq T \end{cases} \quad (21)$$

Also, current flowing through capacitor  $C_1$  can be written as:

$$I_{C1}(t) = \begin{cases} \frac{V_{UC} - V_C - 3V_D}{R_{BN}} = \frac{\overline{I_{UC}}}{2} & 0 \leq t \leq kT \\ -\frac{V_{Bat} + 2V_C - 4V_D}{R_{Bf}} = -\overline{I_{Bat}} & kT \leq t \leq T \end{cases} \quad (22)$$

Here,

$$R_{BN} = 3r_s + r_c \quad R_{Bf} = 4r_s + 2r_c$$

$\overline{I_{UC}}$  is the average input current during the switch-on period,  $kT$ , and  $\overline{I_{Bat}}$  is the average output current during the switch-off period,  $(1-k)T$ . The voltage across capacitor  $C_1$  can be written as:

$$V_C = \frac{kR_{Bf}(V_{UC} - 3V_D) + 2(1-k)R_{BN}(V_{Bat} + 4V_D)}{4(1-k)R_{BN} + kR_{Bf}} \quad (23)$$

Upon determining the total input and output power, the overall transfer efficiency can be computed as:

$$\eta = \frac{P_O}{P_I} = \frac{V_{Bat} * [(1-k) * (\frac{-V_{Bat} + 2V_C - 4V_D}{R_{Bf}})]}{V_{UC} * k * (\frac{V_{UC} - V_C - 3V_D}{R_{BN}})} \quad (24)$$

In boost mode (or codes 3 and 4), the battery modules are fully discharged and the UC modules are half charged or fully charged. Therefore, transfer efficiency in boost mode, with total battery voltage 59.9V and UC voltage 35V, is computed to be around 86%.

## VI. CONCLUSIONS AND FUTURE WORK

This paper presents the performance comparison and transfer efficiency modeling and analysis of a 4-Q SC *Luo* converter and 2-Q SCC, applicable for HEV/PHEV ESS applications. SCCs offer essential features of voltage step-down, voltage step-up, and bidirectional power flow, associated with two or more HEV energy storage devices. It is clear, that for HEV energy storage applications, the 4-Q SC *Luo* converter has transfer efficiencies higher than those for the SCC. This is due to the fact that, in the SC *Luo* converter during buck and boost mode uses the *current-amplification technique* and *voltage-lift technique*, respectively. As a result, reduced overall losses can be experienced, and the resulting efficiency is enhanced.

Future work includes hardware-in-the-loop (HIL) implementation of the 4-Q SC *Luo* converter topology with the proposed novel control strategy, for EV/HEV dual energy storage systems (ESS), running on various driving load patterns.

## REFERENCES

- [1] Z. Amjadi and S. S. Williamson, "Power-electronics-based solutions for plug-in hybrid electric vehicle energy storage and management systems," *IEEE Transactions on Industrial Electronics*, vol. 57, no. 2, pp. 608-616, Feb. 2010.
- [2] A. Emadi, Y. J. Lee, and K. Rajashekara, "Power electronics and motor drives in electric, hybrid electric, and plug-in hybrid electric vehicles," *IEEE Trans. on Industrial Electronics*, vol. 55, no. 6, pp. 2237-2245, June 2008.
- [3] Z. Amjadi and S. S. Williamson, "A novel control technique for a switched capacitor converter based hybrid electric vehicle energy storage system," *IEEE Transactions on Industrial Electronics*, vol. 57, no. 3, pp. 926-934, Feb. 2010.
- [4] F. L. Luo and H. Ye, *Advanced DC/DC Converters*, CRC Press, Boca Raton, FL, 2004.
- [5] S. M. Lukic and A. Emadi, "Charging ahead," *IEEE Industrial Electronics Society Magazine*, vol. 2, no. 4, pp. 22-31, Dec. 2008.
- [6] X. Yan and D. Patterson, "Improvement of drive range, acceleration and deceleration performances in an electric vehicle propulsion system," in *Proc. IEEE Power Electronics Specialists Conf.*, June 1999, vol. 2, pp. 638-643.
- [7] A. Affanni, A. Bellini, G. Franceschini, P. Guglielmi, and C. Tassoni, "Battery choice and management for new-generation electric vehicles," *IEEE Trans. on Industrial Electronics*, vol. 52, no. 5, pp. 1343-1349, Oct. 2005.
- [8] A. F. Burke, "Batteries and ultra-capacitors for electric, hybrid, and fuel cell vehicles," *Proc. of the IEEE*, vol. 95, no. 4, pp. 806-820, April 2007.
- [9] M. Veerachary and N. T. Reddy "Voltage-mode control of hybrid switched capacitor converters," in *Proc. IEEE Industrial Electronics Conf.*, Nov. 2006, pp. 2450-2453.
- [10] A. C. Baughman and M. Ferdowsi, "Double-tiered switched-capacitor battery charge equalization technique," *IEEE Trans. on Industrial Electronics*, vol. 55, no. 6, pp. 2277-2285, June 2008.
- [11] H. Chung, O. Brian, and A. Ioinovici, "Switched-capacitor-based DC-DC converter with improved input current waveform," in *Proc. IEEE International Symp. on Circuits and Systems*, May 1996, Atlanta, GA, vol. 1, pp. 541-544.
- [12] O. C. Mak and A. Ioinovici, "Switched-capacitor inverter with high power density and enhanced regulation capability," *IEEE Trans. on Circuits Systems*, vol. 45, no. 4, pp. 336-347, April 1998.
- [13] H. Chung and Y. K. Mok, "Inductorless DC/DC boost converter using switched-capacitor circuit," in *Proc. IEEE International Symp. on Circuits and Systems*, June 1997, vol. 2, pp. 925-928.
- [14] H. S. H. Chung, W. C. Chow, S. Y. R. Hui, and S. T. S. Lee, "Development of a switched-capacitor DC-DC converter with bidirectional power flow," *IEEE Trans. on Circuits and Systems*, vol. 47, no. 9, pp. 1383-1389, Sept. 2000.
- [15] F. L. Luo, "Luo converters, voltage lift technique," in *Proc. IEEE Power Electronics Specialists Conf.*, Fukuoka, Japan, May 1998, pp. 1783-1789.
- [16] F. L. Luo, "Luo-converters, a series of new DC-DC step-up (boost) conversion circuits," in *Proc. IEEE International Conf. on Power Electronics and Drive Systems*, May 1997, vol. 2, pp. 882-888.
- [17] F. L. Luo, "Negative output *Luo* converters: voltage lift technique," *IEE Proc. on Electric Power Applications*, vol. 146, no. 2, pp. 208-223, March 1999.
- [18] F. L. Luo, "Re-lift circuit: a new DC-DC step-up (boost) converter," *IEEE Electronics Letters*, vol. 33, no. 1, pp. 5-7, Jan. 1997.